OPEN

# Thrombospondin 2 drives liver metastasis in skin cutaneous melanoma via regulation of angiogenesis and extracellular matrix remodeling

Li-Ping Zhang[a], Zhen-Guo Zhang[a], Jian Guan[a] and Li-Qun Li[b]

**To explore the functional role of thrombospondin 2 (THBS2) in the metastasis of skin cutaneous melanoma (SKCM), with a focus on its regulation of angiogenesis and extracellular matrix (ECM) remodeling. THBS2 expression was assessed in normal melanocytes and SKCM cell lines with varying metastatic potential. Functional analyses were conducted after THBS2 knockdown in A375 cells and overexpression in G-361 cells. Effects on migration, invasion, endothelial tube formation, and angiogenesis- and ECM-related factors were evaluated. Tumor IMmune Estimation Resource database was used for correlation analyses in SKCM samples. A liver metastasis model was established by intrasplenic injection of B16-F10 cells into Thbs2 knockout and wild-type mice, followed by quantification of hepatic metastases and molecular analysis of peritumoral liver tissue. THBS2 was highly expressed in invasive melanoma cell lines and was positively associated with VEGFA, PECAM1, and MMPs in both databases and experimental models. Knockdown of THBS2 significantly suppressed VEGFA, PECAM1, FGF2, FLT1, MMP2, MMP9, and ECM components (LAMA4, COL1A1, and COL4A1) at mRNA and protein levels, inhibited melanoma cell migration and invasion, and reduced tube formation in human umbilical vein endothelial cells. Overexpression had opposite effects. *In vivo*, Thbs2 knockout mice exhibited significantly fewer hepatic metastases and reduced metastatic area compared with wild-type controls. Expression of Lama4, Pecam1, Vegfa, Mmp2, and Mmp9 was markedly lower in peritumoral liver tissue of knockout mice. THBS2 promotes SKCM metastasis by enhancing angiogenesis and ECM remodeling. Targeting THBS2 may represent a promising strategy for inhibiting melanoma progression and distant organ colonization. *Melanoma Res* 35: 306–316 Copyright © 2025 The Author(s). Published by Wolters Kluwer Health, Inc.**

**Melanoma Research** 2025, **35**:306–316

**Keywords: angiogenesis, extracellular matrix remodeling, liver metastasis, skin cutaneous melanoma, THBS2**

[a]Department of Plastic Surgery, Wenzhou Medical University Lishui Hospital, Lishui People' s Hospital, Lishui and [b]Department of Plastic Surgery, The First Affiliated Hospital of Wenzhou Medical University, Wenzhou, Zhejiang, China

Correspondence to Li-Qun Li, PhD, Department of Plastic Surgery, The First Affiliated Hospital of Wenzhou Medical University, Nanbaixiang Street, Ouhai District, Wenzhou 325000, Zhejiang, China
Tel: +86 13706664412; e-mail: llq_664412@126.com

**Received** 23 April 2025 **Accepted** 16 June 2025.

## Introduction

Skin cancer is the most frequently diagnosed malignancy worldwide, with melanoma accounting for approximately 20% of all skin cancer cases and an estimated 325 000 new diagnoses globally in 2020 [1]. First introduced by René Laennec in 1812, the term 'melanoma' refers to a malignancy originating from melanocytes, most commonly occurring in the skin cutaneous melanoma (SKCM), but also arising in noncutaneous sites such as the uvea, gastrointestinal tract, genitalia, urinary tract, and meninges [2]. The development of SKCM is influenced by a range of intrinsic and extrinsic risk factors, including skin phototype, genetic susceptibility, immune status, ultraviolet radiation exposure, and sunburn history [2]. While early-stage melanoma can often be effectively managed by surgical resection, advanced disease is characterized by frequent distant metastases – particularly to visceral organs such as the liver [3]. Melanoma metastasis involves complex interactions between tumor cells and their microenvironment, including angiogenesis, extracellular matrix (ECM) remodeling, and immune modulation [4–6]; however, the molecular mechanisms governing hepatic colonization remain incompletely understood.

Thrombospondin 2 (THBS2), encoded by the *THBS2* gene (MIM 188061), is a secreted trimeric matricellular glycoprotein involved in regulating ECM architecture and vascular remodeling [7]. Structurally, THBS2 contains a procollagen-like domain and multiple thrombospondin repeats (TSR1–3), enabling it to interact with both matrix components and cell surface receptors [8]. Its biological roles are context-dependent, spanning normal tissue remodeling to pathological fibrosis, and tumor progression. In dermatological conditions, THBS2 has been implicated in wound repair and fibroblast activation. For example, Song *et al.* [9] demonstrated that THBS2 promotes fibroblast proliferation and migration

in hypertrophic scars through activation of the transforming growth factor beta 1 (TGF-β1)/phosphorylated SMAD2 and SMAD3 signaling pathway, suggesting a role in aberrant ECM accumulation. Conversely, Giunta *et al.* [10] excluded THBS2 as a causal gene in classical Ehlers–Danlos syndrome, indicating that its role in connective tissue disorders may be limited or secondary. Accumulating evidence points to a significant role of THBS2 in cancer biology, particularly through its ability to modulate ECM composition and angiogenic signaling. Mutations in *THBS2* can act in a dominant-negative manner, disrupting ECM homeostasis and promoting tumor cell dissemination [7]. THBS2 has been shown to regulate prometastatic traits such as invasion, migration, and angiogenesis across various solid tumors, including colorectal cancer [11], intrahepatic cholangiocarcinoma [8], and mucinous ovarian carcinoma [12]; however, despite its established involvement in these malignancies, the specific function of THBS2 in melanoma metastasis – especially in the hepatic microenvironment – remains poorly defined.

In this study, we aimed to elucidate the functional role of THBS2 in melanoma metastasis. By combining in-vitro cellular assays, transcriptomic profiling, and an in-vivo liver metastasis model using *Thbs2*-deficient mice, we demonstrate that THBS2 promotes melanoma cell invasion, angiogenesis, and ECM remodeling. Our findings reveal that THBS2 facilitates liver colonization by creating a prometastatic niche and identify it as a potential therapeutic target in the management of advanced melanoma.

## Materials and methods

### Ethics statement

All animal experiments were approved by the Ethics Committee of our hospital and conducted in accordance with the National Institutes of Health Guide for the Care and Use of Laboratory Animals [13].

### Tumor IMmune Estimation Resource database analysis

To investigate the differential expression of THBS2 between primary and metastatic melanoma, we utilized the Tumor IMmune Estimation Resource (TIMER) database, https://cistrome.shinyapps.io/timer/), a web server for comprehensive analysis of tumor-infiltrating immune cells [14]. The SKCM dataset was selected, and THBS2 mRNA expression levels were compared between primary tumor samples ($n$ = 103) and metastatic tumor samples ($n$ = 368).

### Cell culture

Primary adult human epidermal melanocytes (HEMa; PCS-200-013) were cultured in dermal cell basal medium supplemented with the Adult Melanocyte Growth Kit (PCS-200-042). Human melanoma cell lines, including Roswell Park Memorial Institute (RPMI)-7951 (HTB-66), SK-MEL-28 (HTB-72), and MeWo (HTB-65), were maintained in Eagle's minimum essential medium (30-2003) with 10% fetal bovine serum (FBS; 30-2020). A375 (CRL-1619) and B16-F10 (CRL-6475) cells were cultured in Dulbecco' s modified Eagle' s medium (DMEM, 30-2002) with 10% FBS, and G-361 (CRL-1424) cells were maintained in McCoy's 5a medium modified (30-2007) supplemented with 10% FBS. Human umbilical vein endothelial cells (HUVECs; PCS-100-013) were cultured in vascular cell basal medium (PCS-100-030) supplemented with the Endothelial Cell Growth Kit-BBE (PCS-100-040). The final complete medium contained 2% FBS, 0.2% bovine brain extract, 5 ng/ml epidermal growth factor , 10 mM L-glutamine, 0.75 U/ml heparin, 1 µg/ml hydrocortisone hemisuccinate, and 50 µg/ml ascorbic acid. All cells (from ATCC, Manassas, Virginia, USA) were maintained at 37 °C in a humidified incubator with 5% $CO_2$, and the medium was changed every 2–3 days.

### Cell grouping and transfection

Cells were divided into two experimental groups. Group 1 (A375 cells): A375-mock, A375-shCtrl, and A375-shTHBS2. THBS2 knockdown was achieved using THBS2 short hairpin RNA (shRNA) plasmid (sc-37031-SH; Santa Cruz Biotechnology, Dallas, Texas, USA) with corresponding plasmid transfection reagent (sc-108061) and transfection medium (sc-108062). A nontargeting control shRNA plasmid (shCtrl, sc-108060) was used as a negative control. Group 2 (G-361 cells): G-361-mock, G-361-vector, and G-361-THBS2. THBS2 overexpression was performed using THBS2 lentiviral activation particles (sc-401207-LAC; Santa Cruz Biotechnology), with corresponding control lentiviral activation particles (control vector, sc-437282). Cells were incubated for 48 h posttransfection or infection before quantitative real-time PCR (qRT-PCR) and western blot analyses.

### Cell invasion assay

Cells (A375 and G-361) were cultured to approximately 70–80% confluence before invasion assays. Corning BioCoat Matrigel invasion chambers (24-well format) were thawed at room temperature for approximately 1 h. Upper and lower chambers were rehydrated with 500 µl serum-free RPMI medium for 2 h at 37 °C. Subsequently, cells were seeded at $5 \times 10^5$ cells/ml in the upper chamber (500 µl), while 20% FBS-containing RPMI medium was added to the lower chamber as a chemoattractant. After incubation at 37 °C for 24 h, noninvasive cells were gently removed from the upper membrane surface. Cells invading through the membrane were fixed and stained with 0.25% crystal violet solution. After washing, stained cells were dissolved with dimethyl sulfoxide, and absorbance was measured at 560 nm. Each experimental

**Table 1 Primer sequences used in quantitative real-time PCR**

| Genes | Species | Forward primer (5′→3′) | Reverse primer (5′→3′) |
|---|---|---|---|
| *VEGFA* | Human | AGGGCAGAATCATCACGAAGT | AGGGTCTCGATTGGATGGCA |
| *FGF2* | Human | AGAAGAGCGACCCTCACATCA | CGGTTAGCACACACTCCTTTG |
| *PECAM1* | Human | AACAGTGTTGACATGAAGAGCC | TGTAAAACAGCACGTCATCCTT |
| *FLT1* | Human | TTTGCCTGAAATGGTGAGTAAGG | TGGTTTGCTTGAGCTGTGTTC |
| *FN1* | Human | CGGTGGCTGTCAGTCAAAG | AAACCTCGGCTTCCTCCATAA |
| *LAMA4* | Human | GCAGTGGAAATTCAGATCCCA | TAACCGCAGGTCATCAGTCAG |
| *COL1A1* | Human | GAGGGCCAAGACGAAGACATC | CAGATCACGTCATCGCACAAC |
| *COL4A1* | Human | GGACTACCTGGAACAAAAGGG | GCCAAGTATCTCACCTGGATCA |
| *MMP2* | Human | TACAGGATCATTGGCTACACACC | GGTCACATCGCTCCAGACT |
| *MMP9* | Human | TGTACCGCTATGGTTACACTCG | GGCAGGGACAGTTGCTTCT |
| *GAPDH* | Human | GGAGCGAGATCCCTCCAAAAT | GGCTGTTGTCATACTTCTCATGG |
| *Lama4* | Mouse | ATGAGCTGCAAGGAAAACTATCC | CTGTTTCGTTGGCTTCACTGA |
| *Pecam1* | Mouse | CTGCCAGTCCGAAAATGGAAC | CTTCATCCACCGGGGCTATC |
| *Vegfa* | Mouse | GCACATAGAGAGAATGAGCTTCC | CTCCGCTCTGAACAAGGCT |
| *Mmp2* | Mouse | CAAGTTCCCCGGCGATGTC | TTCTGGTCAAGGTCACCTGTC |
| *Mmp9* | Mouse | CTGGACAGCCAGACACTAAAG | CTCGCGGCAAGTCTTCAGAG |
| *Gapdh* | Mouse | AGGTCGGTGTGAACGGATTTG | TGTAGACCATGTAGTTGAGGTCA |

*COL1A1*, collagen type I alpha 1 chain; *COL4A1*, collagen type IV alpha 1 chain; *FGF2*, fibroblast growth factor 2; *FLT1*, fms-related tyrosine kinase 1 (*VEGFR1*); *FN1*, fibronectin 1; *GAPDH*/*Gapdh*, glyceraldehyde-3-phosphate dehydrogenase); *LAMA4*, laminin subunit alpha 4; *MMP2*, matrix metallopeptidase 2; *MMP9*, matrix metallopeptidase 9; *PECAM1*, platelet/endothelial cell adhesion molecule 1 (also known as CD31); *VEGFA*, vascular endothelial growth factor A.

condition was repeated three times independently, and data were expressed as relative absorbance normalized to the mock group.

### Wound healing assay

Cells (A375 and G-361) were seeded into 24-well plates and cultured until 70–80% confluence. The cell monolayer was gently scratched using a sterile 1-ml pipette tip to create a cross-shaped wound. After carefully washing twice with medium to remove detached cells, fresh medium was added. Cells were further cultured for 48 h. Cells were fixed in 3.7% paraformaldehyde (30 min), stained with 1% crystal violet (in 2% ethanol) for 30 min, and photographed using an inverted microscope. Image J software was used to quantitatively assess the extent of wound closure. The percentage of wound closure was calculated by comparing the area of the wound at 24 h with the initial area at 0 h. Experiments were performed in triplicate.

### In-vitro human umbilical vein endothelial cell tube-formation assay

A375 and G-361 cells were cultured until 30–40% confluent, switched to serum-free DMEM, and cultured for an additional 24 h to generate conditioned media, which were stored at −80 °C. HUVECs were cultured in medium 200PRF supplemented with low serum growth supplement until 70–80% confluent, then starved for 3–6 h. Growth factor-reduced Matrigel (50 µl) was added to precooled 96-well plates and polymerized at room temperature for 1 h. HUVECs ($4 \times 10^5$ cells/ml) were then suspended in the collected conditioned media supplemented with 1% FBS and seeded onto Matrigel-coated wells (100 µl/well). After 12 h incubation at 37 °C, capillary-like structures were photographed under an inverted microscope, and tube length was analyzed using imaging software. The number of tubes was quantified and compared across experimental groups. Experiments were performed in triplicate.

### Animals

Thbs2 knockout (Strain #: 006238) and wild-type (Strain #: 000664) female mice, both on a C57BL/6J background, were obtained from The Jackson Laboratory (Bar Harbor, Maine, USA). At 11 weeks of age, mice were administered intrasplenic injections of B16-F10 melanoma cells ($1.5 \times 10^5$ cells/mouse). Two weeks later, animals were euthanized, and livers were harvested for metastasis evaluation. The number of macroscopically visible liver metastases was recorded. Peritumoral liver tissues were collected, snap-frozen in liquid nitrogen, and stored at −80 °C for subsequent qRT-PCR and western blot analyses. Expression levels of angiogenesis- and matrix remodeling-related genes and proteins – including Lama4, Pecam1 (CD31), Vegfa, Mmp2, and Mmp9 – were measured.

### Quantitative real-time PCR

Total RNA was extracted from cultured cells or tissue samples using TRIzol Reagent (Invitrogen, Carlsbad, California, USA) according to the manufacturer's instructions. RNA concentration and purity were assessed using a NanoDrop spectrophotometer. Real-time quantitative RT-PCR was performed using the SuperScript III Platinum SYBR Green One-Step qRT-PCR Kit (Invitrogen). Reaction mixtures (50 µl) were prepared on ice containing 25 µl 2X SYBR Green reaction mix, 1 µl SuperScript III RT/Platinum Taq mix, 1 µl each of forward and reverse primers (10 µM), 0.1 µl 6-carboxy-x-rhodamine reference dye, RNA template, and diethyl pyrocarbonate -treated water. qRT-PCR was performed on an ABI 7500 Fast real-time PCR system with the following cycling conditions: reverse transcription at 50 °C for 5 min, initial denaturation at 95 °C

for 2 min, followed by 40 cycles of 95 °C for 3 s and 60 °C for 30 s. Primer sequences were listed in Table 1. GAPDH was used as an internal control for normalization. All experiments were performed in triplicate, and results were analyzed using appropriate software.

### Western blotting

Total protein was extracted from cells and tissues using radio-immunoprecipitation assay lysis buffer (sc-24948) containing protease inhibitors. Lysates were sonicated and centrifuged at high speed (14 000 rpm) at 4 °C to remove insoluble materials. Protein concentration was determined using a bicinchoninic acid assay. Protein samples were boiled at 95–100 °C in loading buffer containing dithiothreitol for 10 min, separated by SDS-PAGE, and transferred to an activated polyvinylidene fluoride membrane (sc-3723). Membranes were blocked with 5% skim milk or BSA for 1 h at room temperature and incubated overnight at 4 °C with primary antibodies. Membranes were then incubated for 1 h at room temperature with horse-radish peroxidase-conjugated secondary antibodies. Protein bands were visualized using enhanced chemiluminescence and quantified by imaging software. All experiments were independently repeated three times.

### Statistical analysis

All data are presented as mean ± SD. Statistical significance was assessed using unpaired two-tailed Student's *t* test for comparisons between two groups, and one-way analysis of variance (ANOVA) followed by Holm–Sidak's multiple comparisons test for comparisons among multiple groups. A $P$ value less than 0.05 was considered statistically significant. All statistical analyses were performed using GraphPad Prism software.

## Results

### Differential expression of thrombospondin 2 in melanoma cell lines and its association with metastasis

Previous research employing a reconstructed human melanoma-in-skin model demonstrated varying invasive capabilities among melanoma cell lines, where A375 showed the highest invasive phenotype; SK-MEL-28, G361, and MeWo displayed moderate invasion; and RPMI-7951 exhibited minimal invasive potential [15]. To investigate the potential involvement of THBS2 in melanoma invasion and metastasis, we assessed THBS2 mRNA and protein expression in normal melanocytes (HEMa) and melanoma cell lines (RPMI-7951, SK-MEL-28, G-361, MeWo, and A375). Quantitative RT-PCR revealed significantly higher THBS2 mRNA levels in RPMI-7951 ($P = 0.030$), G-361 ($P = 0.007$), MeWo ($P < 0.001$), SK-MEL-28 ($P < 0.001$), and A375 ($P < 0.001$), relative to HEMa (Fig. 1a). Western blot analysis confirmed this trend at the protein level, with marked upregulation in RPMI-7951 ($P = 0.010$), G-361 ($P = 0.008$), MeWo ($P < 0.001$), SK-MEL-28 ($P < 0.001$), and A375 ($P < 0.001$), compared with HEMa (Fig. 1b and c). The two cell lines with the highest invasive potential (A375 and SK-MEL-28) exhibited the greatest THBS2 expression at both mRNA and protein levels, without statistically significant differences between them ($P > 0.05$). Similarly, G-361 and RPMI-7951, characterized by moderate or lower invasive potential, displayed intermediate THBS2 expression levels that did not differ significantly ($P > 0.05$). In addition, analysis of melanoma expression data from the TIMER database indicated a significant upregulation of THBS2 in metastatic melanoma samples ($n = 368$) compared with primary melanomas ($n = 103$) ($P < 0.001$, Fig. 1d). On the basis of these data, we selected A375 cells (high THBS2 expression) for gene knockdown (Fig. 1e–g) and G-361 cells (moderate THBS2 expression) for overexpression studies (Fig. 1h–j). THBS2 knockdown significantly reduced THBS2 levels in A375-shTHBS2 cells ($P < 0.001$), whereas THBS2 overexpression markedly increased its levels in G-361-THBS2 cells ($P < 0.001$), demonstrating successful genetic manipulation.

### Thrombospondin 2 promotes melanoma angiogenesis through upregulation of angiogenesis-related factors

Correlation analysis using the TIMER database demonstrated significant positive correlations between THBS2 and angiogenesis-associated genes VEGFA, FGF2, PECAM1, and FLT1 in both primary ($n = 103$, Fig. 2a) and metastatic melanoma samples ($n = 369$, Fig. 2b). Specifically, in primary melanoma, THBS2 expression positively correlated with VEGFA ($r = 0.217$, $P < 0.001$), FGF2 ($r = 0.383$, $P < 0.001$), PECAM1 ($r = 0.420$, $P < 0.001$), and FLT1 ($r = 0.489$, $P < 0.001$). Similar trends were observed in metastatic melanoma tissues, with significant positive correlations between THBS2 and VEGFA ($r = 0.208$, $P < 0.001$), FGF2 ($r = 0.399$, $P < 0.001$), PECAM1 ($r = 0.421$, $P < 0.001$), and FLT1 ($r = 0.503$, $P < 0.001$). To experimentally validate these correlations, we performed qRT-PCR and western blotting analysis and found that knockdown of THBS2 significantly decreased expression levels of VEGFA, FGF2, PECAM1, and FLT1 in A375-shTHBS2 cells (all $P < 0.05$, Fig. 2c and d). Conversely, THBS2 overexpression markedly enhanced the levels of these angiogenesis-related factors in G-361-THBS2 cells (all $P < 0.05$; Fig. 2e and f). To further assess the functional relevance, tube formation assays were performed using conditioned media from genetically manipulated melanoma cells (Fig. 2g and h). The conditioned medium from A375-shTHBS2 cells led to a significant reduction in the number of tubes formed by HUVECs compared with controls ($P < 0.05$), whereas medium from G-361-THBS2 cells significantly promoted tube formation ($P < 0.05$). These results collectively suggest that THBS2 promotes melanoma angiogenesis by modulating the expression of key proangiogenic factors.

**Fig. 1**

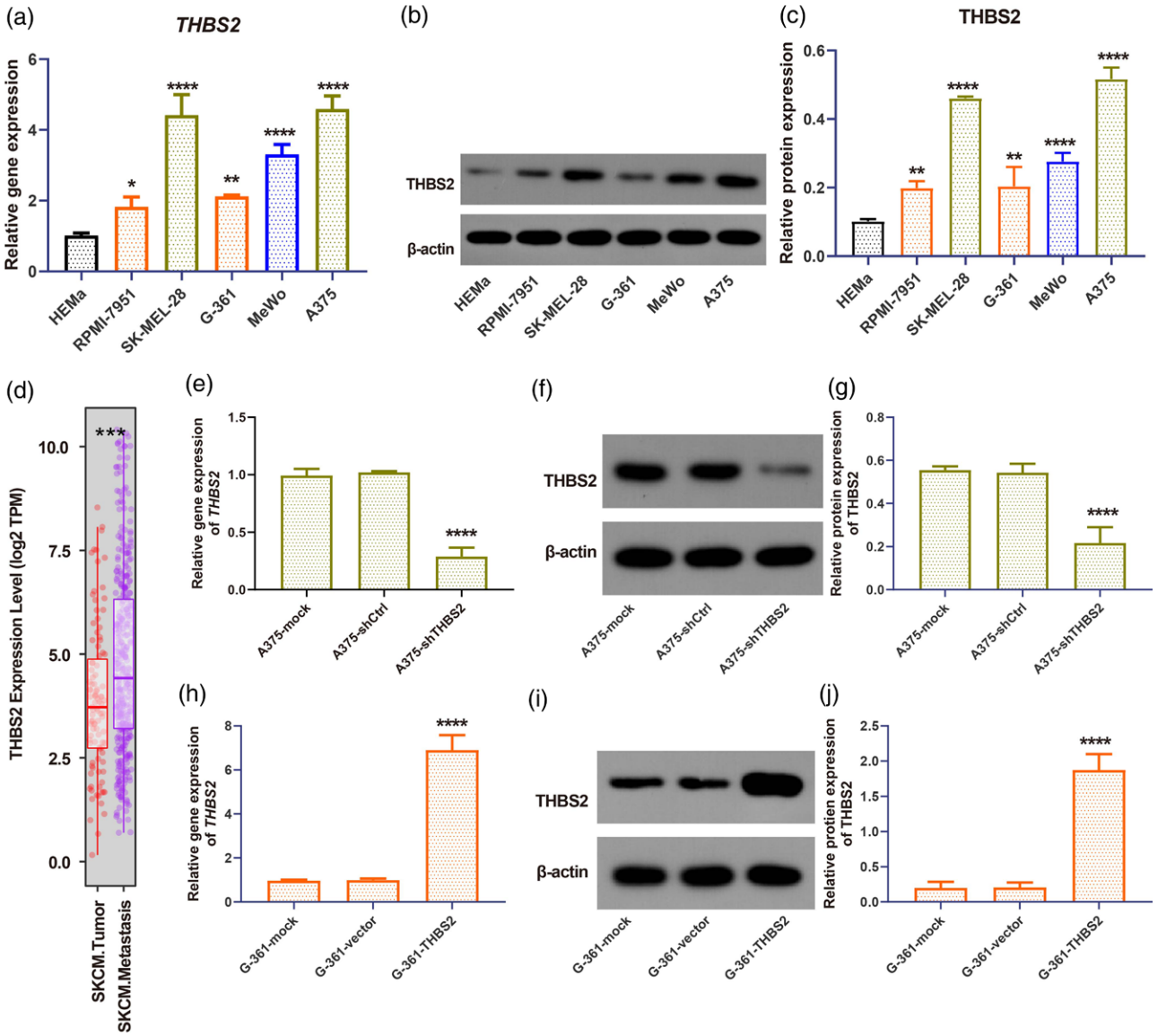


THBS2 expression profiles in melanoma cell lines and genetic manipulation validation. (a) qRT-PCR analysis of THBS2 mRNA levels in normal melanocytes (HEMa) and melanoma cell lines (RPMI-7951, SK-MEL-28, G-361, MeWo, and A375). (b and c) Western blotting images and quantification of THBS2 protein expression normalized to β-actin. Data are shown as mean ± SD; $^{*}P < 0.05$, $^{**}P < 0.01$, $^{***}P < 0.005$, $^{****}P < 0.001$ versus HEMa cells. (d) Analysis of THBS2 expression data from the TIMER database shows significantly higher levels in metastatic melanomas ($n = 368$) compared with primary melanomas ($n = 103$), indicating a correlation with metastasis. (e–g) THBS2 knockdown in A375 cells confirmed by qRT-PCR (e) and western blotting analysis (f and g); $^{****}P < 0.001$ versus A375-mock control. (h–j) THBS2 overexpression in G-361 cells validated by qRT-PCR (h) and western blot analysis (i and j); $^{****}P < 0.001$ versus G-361-mock control. Data represent mean ± SD from three independent experiments. HEMa, human epidermal melanocyte; qRT-PCR, quantitative real-time PCR; RPMI, Roswell Park Memorial Institute; THBS2, thrombospondin 2; TIMER, Tumor Immune Estimation Resource.

### Thrombospondin 2 promotes melanoma cell invasion and migration via extracellular matrix remodeling and matrix metallopeptidase regulation

Previous transcriptomic profiling of murine melanoma models with distinct hepatic metastatic capacities identified THBS2 as one of the most significantly upregulated genes in highly metastatic lines, closely associated with ECM remodeling and MMPs activity [16]. In our study, Transwell invasion assays demonstrated that THBS2 knockdown significantly reduced the invasive capacity of A375 cells compared with controls ($P < 0.05$), whereas THBS2 overexpression in G-361 cells significantly enhanced invasion ($P < 0.01$, Fig. 3a and d). Similarly, wound healing assays showed that THBS2 silencing in A375 led to reduced migratory ability at 24 h ($P < 0.01$), while THBS2 overexpression promoted G-361 cell

**Fig. 2**

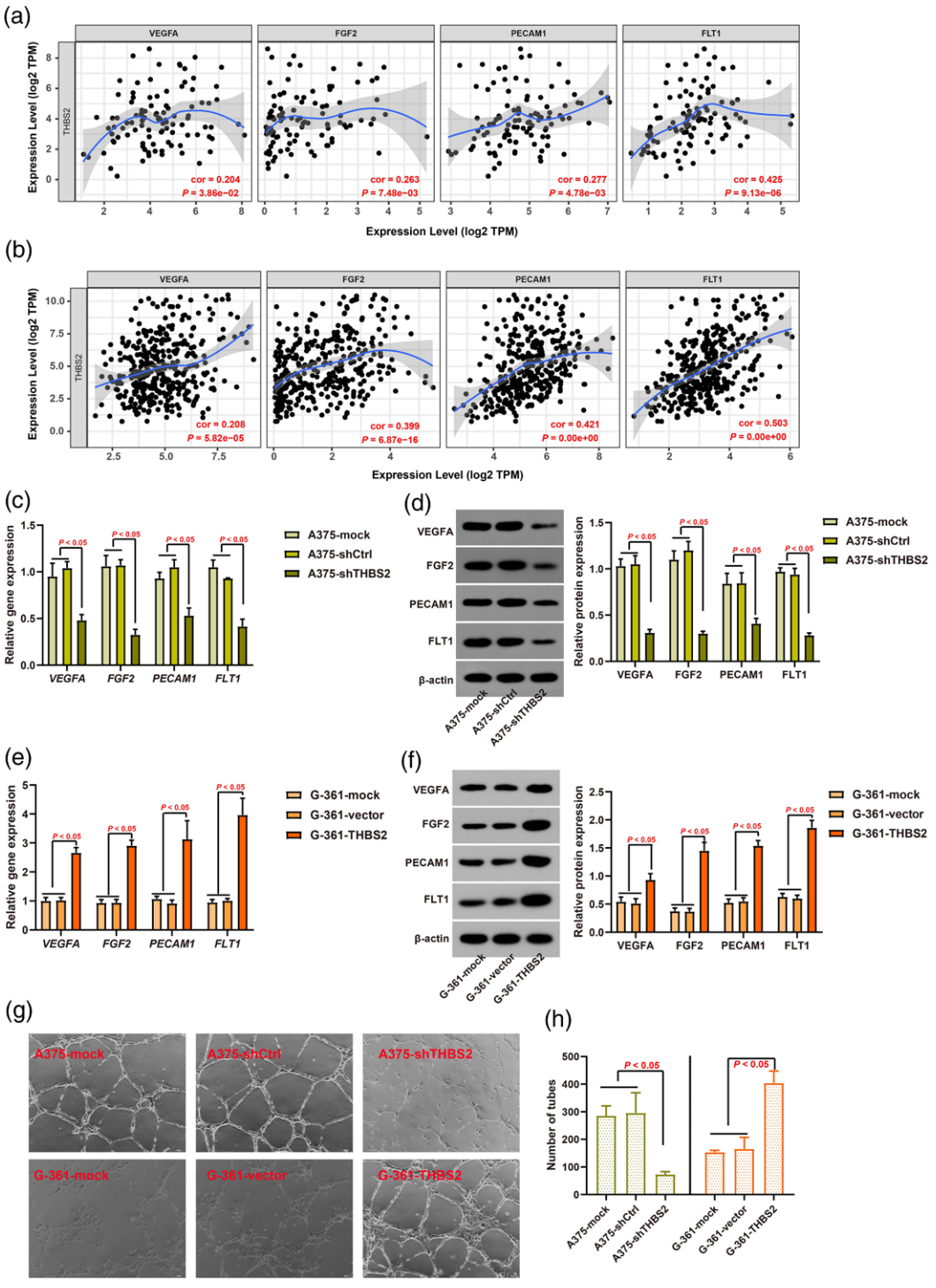


THBS2 enhanced angiogenesis in melanoma through upregulation of angiogenesis-related factors. (a and b) Correlation analysis of THBS2 with angiogenesis-associated genes *VEGFA*, *FGF2*, PECAM1, and FLT1 in primary melanoma (a) and metastatic melanoma (b) using the TIMER database. (c–f) Relative mRNA and protein expression of VEGFA, FGF2, PECAM1, and FLT1 in A375 cells with THBS2 knockdown (c and d) and G-361 cells with THBS2 overexpression (e and f), assessed by qRT-PCR and western blotting. (g and h) Representative images (g) and quantification (h) of tube formation in HUVECs cultured in conditioned media derived from melanoma cells with altered THBS2 expression. Data represent mean ± SD from three independent experiments. *FGF2*, fibroblast growth factor 2; *FLT1*, Fms-related tyrosine kinase 1; HUVECs, human umbilical vein endothelial cells; *PECAM1*, platelet and endothelial cell adhesion molecule 1; qRT-PCR, quantitative real-time PCR; THBS2, thrombospondin 2; TIMER, Tumor Immune Estimation Resource; *VEGFA*, vascular endothelial growth factor A.

**Fig. 3**

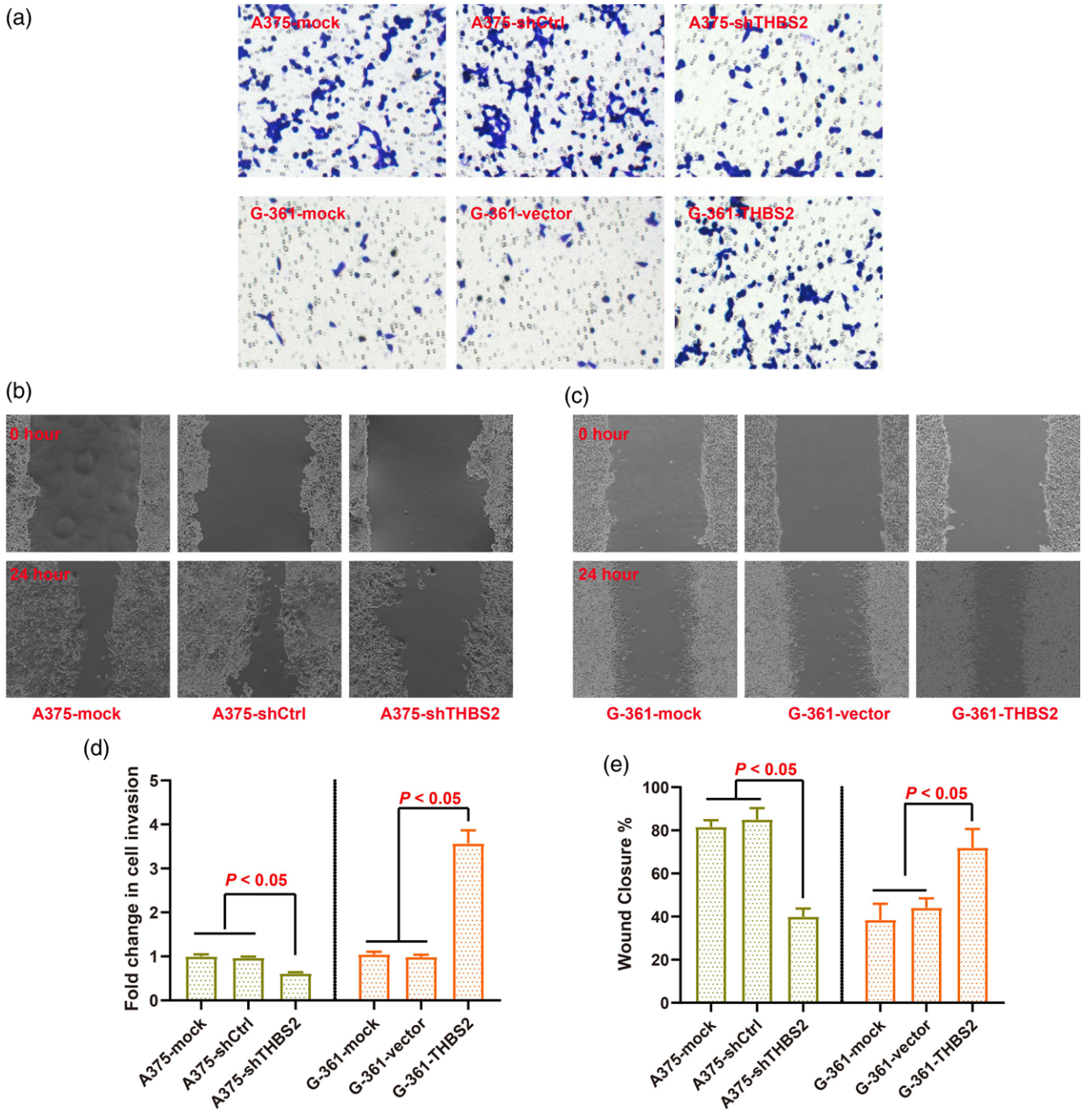


THBS2 regulated melanoma cell invasion and migration in-vitro. (a–c) Representative images of Transwell invasion assays (a) and wound healing assays at 0 and 24 h (b and c) in A375 cells with THBS2 knockdown and G-361 cells with THBS2 overexpression. (d) Fold change in invasive cell number relative to the mock group. (e) Quantification of wound closure percentage at 24 h. Data represent mean ± SD of three independent experiments. THBS2, thrombospondin 2.

migration ($P < 0.05$; Fig. 3b, c, and e). To further explore the molecular mechanisms involved, we analyzed the correlation between THBS2 and key ECM-related genes and MMPs using the TIMER database. In primary melanoma samples, THBS2 expression was significantly positively correlated with LAMA4 ($r = 0.278$, $P = 0.005$), COL1A1 ($r = 0.414$, $P < 0.001$), COL4A1 ($r = 0.371$, $P < 0.001$), and MMP2 ($r = 0.258$, $P = 0.009$) but not with FN1 or MMP9 ($P > 0.05$) (Fig. 4a). In metastatic samples ($n = 369$), THBS2 exhibited significant positive correlations with all six genes examined, including FN1, LAMA4, COL1A1, COL4A1, MMP2, and

**Fig. 4**

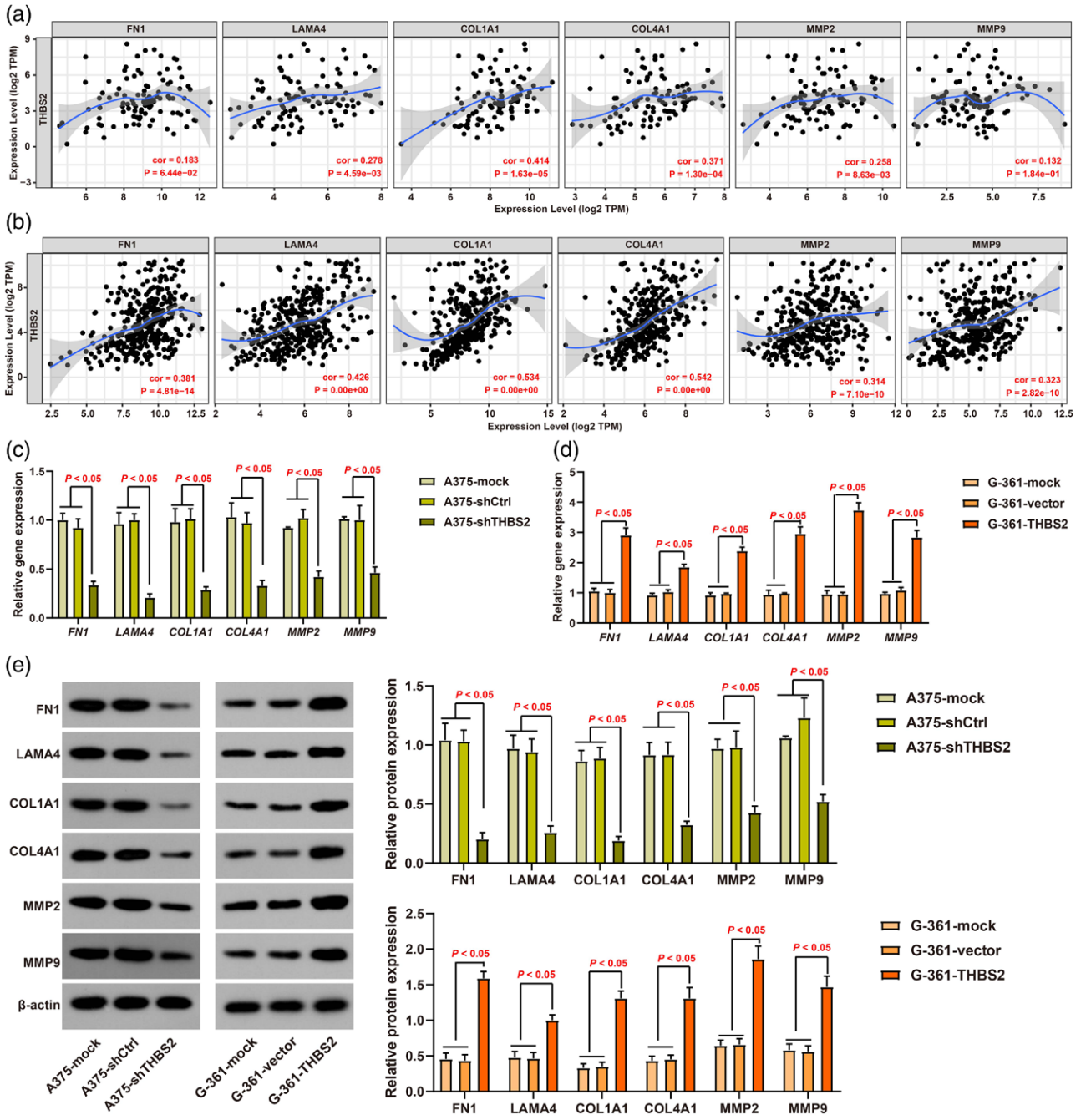


THBS2 was associated with ECM-related gene expression and MMP activity in melanoma. (a and b) Correlation analysis between THBS2 and ECM- or MMP-related genes in primary (a) and metastatic (b) SKCM samples from the TIMER database. (c) qRT-PCR analysis of ECM-related genes and MMPs in A375 cells with THBS2 knockdown (c) and G-361 cells with THBS2 overexpression (d). (e) Western blotting analysis of ECM- and MMP-related protein expressions in A375 and G-361 cells following THBS2 knockdown or overexpression, respectively. Data are presented as mean ± SD from three independent experiments. COL1A1, collagen type I alpha 1 chain; COL4A1, collagen type IV alpha 1 chain; ECM, extracellular matrix; FN1, fibronectin 1; LAMA4, laminin subunit alpha-4; MMP2, matrix metallopeptidase 2; MMP9, matrix metallopeptidase 9; qRT-PCR, quantitative real-time PCR; SKCM, skin cutaneous melanoma; THBS2, thrombospondin 2; TIMER, Tumor Immune Estimation Resource.

MMP9 (all $P < 0.001$, Fig. 4b). Consistently, qRT-PCR (Fig. 4c andd) and western blotting (Fig. 4e) analysis confirmed that knockdown of THBS2 in A375 cells significantly decreased the expression of these ECM-related molecules and MMPs ($P < 0.05$), whereas THBS2 overexpression in G-361 cells led to their marked upregulation ($P < 0.05$). Together, these findings suggest that THBS2 may promote melanoma invasion and metastasis

**Fig. 5**

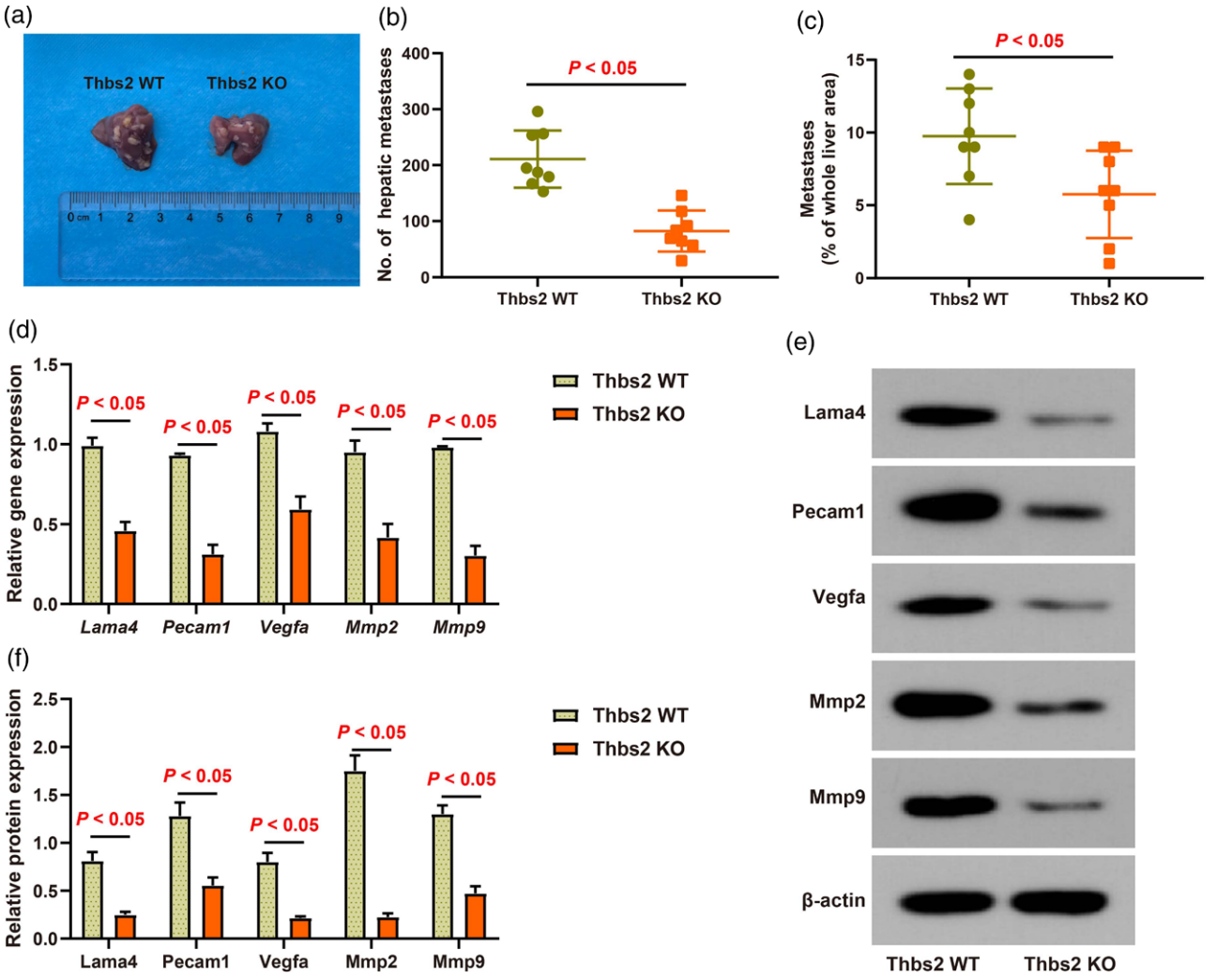


THBS2 deficiency suppressed hepatic melanoma metastasis and downregulated angiogenesis- and ECM-related markers in peritumoral liver tissue. (a) Macroscopic images of representative metastatic livers from Thbs2 WT and KO mice 14 days after intrasplenic injection of B16-F10 cells. (b) Quantification of visible hepatic metastatic nodules. (c) Percentage of liver area occupied by metastases. (d) Relative mRNA expression levels of *Lama4*, *Pecam1*, *Vegfa*, *Mmp2*, and *Mmp9* in peritumoral liver tissues, measured by qRT-PCR. (e and f) Western blotting analysis and quantification of corresponding protein expression in peritumoral liver tissues. Data are shown as mean ± SD; $n = 8$ per group. ECM, extracellular matrix; KO, knockout; qRT-PCR, quantitative real-time PCR; THBS2, thrombospondin 2; WT, wild-type.

by enhancing ECM remodeling and MMP-mediated matrix degradation.

### Thrombospondin 2 deficiency reduces hepatic metastasis and inhibits angiogenesis and extracellular matrix remodeling

To confirm whether the prometastatic effects of THBS2 observed *in vitro* are recapitulated *in vivo*, we utilized a splenic injection model in Thbs2 knockout mice. Consistent with the in-vitro findings, Thbs2 knockout mice exhibited significantly reduced hepatic metastatic burden compared with wild-type controls, as evidenced by a lower number of visible liver metastatic nodules and a decreased percentage of liver area occupied by metastases (both $P < 0.05$; Fig. 5a–c). To further elucidate the molecular changes associated with Thbs2 deficiency, qRT-PCR analysis of peritumoral liver tissue revealed significantly decreased mRNA levels of *Lama4*, *Pecam1*, *Vegfa*, *Mmp2*, and *Mmp9* in knockout mice compared with wild-type (all $P < 0.05$; Fig. 5d). These reductions were also observed at the protein level by western blotting, which showed markedly decreased expression of Lama4, Pecam1, Vegfa, Mmp2, and Mmp9 in the knockout group (all $P < 0.05$; Fig. 5e and f). Together, these data suggest that Thbs2 facilitates melanoma liver metastasis by promoting angiogenesis and ECM remodeling within the tumor microenvironment.

## Discussion

This study identified THBS2 as a key promoter of melanoma metastasis. We found that THBS2 expression was elevated in highly invasive melanoma cell lines and metastatic tissues. Functional analyses revealed that THBS2 enhances melanoma cell migration, invasion, and angiogenesis through the regulation of ECM remodeling and proangiogenic factors. *In vivo*, Thbs2 deficiency significantly reduced liver metastases and suppressed the expression of genes involved in angiogenesis and matrix remodeling, highlighting its critical role in shaping a prometastatic tumor microenvironment.

The observed upregulation of THBS2 in aggressive melanoma cell lines such as A375 and SK-MEL-28, and its enrichment in metastatic melanoma tissues, supports its association with tumor progression. Our findings align with Liu and Ma [17], who reported that THBS2 promotes proliferation and metastasis in uveal melanoma via activation of the phosphoinositide 3-kinase/protein kinase B pathway, thereby enhancing cell invasiveness. Similarly, Wohlfeil *et al.* [16] identified THBS2 among the most upregulated genes in highly liver-metastatic murine melanoma models, suggesting its contribution to hepatic colonization. These studies, together with our own, highlight the broader relevance of THBS2 in melanoma aggressiveness and metastatic potential.

Mechanistically, we demonstrated that THBS2 promotes angiogenesis in melanoma cells. This was supported by its positive correlation with key angiogenesis-related genes (VEGFA, FGF2, PECAM1/CD31, FLT1) and by tube formation assays in HUVECs. These findings are consistent with those in other cancers. For example, Kim *et al.* [18] reported that THBS2 was positively associated with CXCL16-mediated angiogenesis in papillary thyroid cancer. Liu *et al.* [19] showed that THBS2 promotes angiogenesis in colorectal cancer through the HIF1A/lactic acid/GPR132 pathway, enhancing immune suppression and tumor progression. In contrast, Carpino *et al.* [20] and Corbella *et al.* [8] demonstrated that THBS2, alongside THBS1 and PEDF, inhibited angiogenesis but promoted tumor-associated lymphangiogenesis in intrahepatic cholangiocarcinoma. Moreover, Maiti *et al.* [21] found that HDAC inhibitor-induced re-expression of THBS2 suppressed vasculogenic mimicry in triple-negative breast cancer, highlighting its context-dependent role. Taken together, these findings suggest that the angiogenic function of THBS2 is highly tumor-type specific. In the case of melanoma, our data support a proangiogenic role.

In addition to angiogenesis, our data implicate THBS2 as a regulator of ECM remodeling. We observed positive correlations between THBS2 and genes encoding ECM structural proteins (LAMA4, COL1A1, and COL4A1) and MMPs (MMP2 and MMP9), with functional assays confirming that THBS2 promotes cell migration and invasion. This is supported by Abed Kahnamouei *et al.* [22], who found that THBS2 is upregulated during TGF-β-induced epithelial–mesenchymal transition in gastric cancer. Lee *et al.* [23] further identified THBS2 as a desmoplastic fibroblast-derived ECM protein associated with poor prognosis in the mesenchymal subtype of colorectal cancer. Barani *et al.* [24] highlighted THBS2's involvement in ECM–receptor interaction pathways in gastric cancer. Our study expands on these findings by establishing a direct functional link between THBS2 and melanoma invasion through ECM degradation and remodeling, mediated by MMPs.

Our in-vivo experiments provide further validation of THBS2's prometastatic function. Thbs2 knockout mice displayed significantly fewer and smaller hepatic metastases compared with wild-type mice. Furthermore, gene and protein expression analyses in peritumoral liver tissue revealed downregulation of Lama4, Pecam1, Vegfa, Mmp2, and Mmp9 in knockout mice. These changes indicate that THBS2 contributes to creating a liver microenvironment conducive to melanoma cell engraftment, growth, and dissemination. The liver's unique sinusoidal vascular structure and dependence on ECM cues may further potentiate THBS2-mediated metastatic colonization.

Despite the robustness of our findings, several limitations warrant mention. First, while both gain- and loss-of-function approaches were used, the absence of rescue experiments (e.g. re-expression of THBS2 in knockout settings) limits definitive causal conclusions. Second, although gene and protein expression were assessed in peritumoral liver tissue, we did not evaluate tumor-intrinsic changes such as intracellular signaling cascades or tumor–immune interactions. Third, this study relied solely on the B16-F10 murine melanoma model. Whether these findings can be extrapolated to other metastatic organs or to human melanoma remains to be tested. Lastly, our focus on angiogenesis and ECM remodeling does not preclude the involvement of additional THBS2-mediated processes such as immune suppression, exosomal communication, or metabolic reprogramming – all of which merit further investigation.

### Conclusion

In summary, our findings reveal that THBS2 plays a critical role in melanoma progression by enhancing angiogenesis and ECM remodeling, both *in vitro* and *in vivo*. These results position THBS2 as a potential biomarker of metastasis and a candidate target for therapeutic intervention in metastatic melanoma.

## Acknowledgements

This study was funded by the Lishui Science and Technology Bureau (Grant No. 2023GYX64).

L.-P.Z. and Z.-G.Z. performed experiments and data analysis. J.G. assisted in animal experiments and imaging. L.-Q.L. conceived the study, supervised the project, and revised the manuscript. All authors reviewed and approved the final manuscript.

All animal experiments were approved by the Ethics Committee of Wenzhou Medical University Lishui Hospital and conducted in accordance with the National Institutes of Health Guide for the Care and Use of Laboratory Animals.

The datasets and materials used in this study are available from the corresponding author upon reasonable request.

### Conflicts of interest

There are no conflicts of interest.

## References


1 Arnold M, Singh D, Laversanne M, Vignat J, Vaccarella S, Meheus F, *et al*. Global burden of cutaneous melanoma in 2020 and projections to 2040. *JAMA Dermatol* 2022; **158**:495–503.

2 Strashilov S, Yordanov A. Aetiology and pathogenesis of cutaneous melanoma: current concepts and advances. *Int J Mol Sci* 2021; **22**:6395.

3 Wohlfeil SA, Olsavszky A, Irkens AL, Hafele V, Dietsch B, Straub N, *et al*. Deficiency of stabilin-1 in the context of hepatic melanoma metastasis. *Cancers (Basel)* 2024; **16**:441.

4 Riechers A, Schmidt J, Dettmer K, Oefner P, Jachimczak P, Schneider A, Bosserhoff A-K. Inducing anti-tumor cytokines and an immune response in melanoma by inhibition of MIA using the peptide AR71. *Eur J Dermatol* 2013; **23**:820–825.

5 Dai W, Liu S, Wang S, Zhao L, Yang X, Zhou J, *et al*. Activation of transmembrane receptor tyrosine kinase DDR1-STAT3 cascade by extracellular matrix remodeling promotes liver metastatic colonization in uveal melanoma. *Signal Transduct Target Ther* 2021; **6**:176.

6 Jones NM, Yang H, Zhang Q, Morales-Tirado VM, Grossniklaus HE. Natural killer cells and pigment epithelial-derived factor control the infiltrative and nodular growth of hepatic metastases in an orthotopic murine model of ocular melanoma. *BMC Cancer* 2019; **19**:484.

7 Hadar N, Porgador O, Cohen I, Levi H, Dolgin V, Yogev Y, *et al*. Heterozygous THBS2 pathogenic variant causes Ehlers-Danlos syndrome with prominent vascular features in humans and mice. *Eur J Hum Genet* 2024; **32**:550–557.

8 Corbella E, Fara C, Covarelli F, Porreca V, Palmisano B, Mignogna G, *et al*. THBS1 and THBS2 enhance the in vitro proliferation, adhesion, migration and invasion of intrahepatic cholangiocarcinoma cells. *Int J Mol Sci* 2024; **25**:1782.

9 Song B, Zhu Y, Zhao Y, Wang K, Peng Y, Chen L, *et al*. Machine learning and single-cell transcriptome profiling reveal regulation of fibroblast activation through THBS2/TGFbeta1/P-Smad2/3 signalling pathway in hypertrophic scar. *Int Wound J* 2024; **21**:e14481.

10 Giunta C, Nuytinck L, Raghunath M, Hausser I, De Paepe A, Steinmann B. Homozygous Gly530Ser substitution in COL5A1 causes mild classical Ehlers-Danlos syndrome. *Am J Med Genet* 2002; **109**:284–290.

11 Qu HL, Hasen GW, Hou YY, Zhang CX. THBS2 promotes cell migration and invasion in colorectal cancer via modulating Wnt/beta-catenin signaling pathway. *Kaohsiung J Med Sci* 2022; **38**:469–478.

12 Kobel M, Kang EY, Lee S, Terzic T, Karnezis AN, Ghatage P, *et al*. Infiltrative pattern of invasion is independently associated with shorter survival and desmoplastic stroma markers FAP and THBS2 in mucinous ovarian carcinoma. *Histopathology* 2024; **84**:1095–1110.

13 Council NR. *Guide for the care and use of laboratory animals*. 8th ed. The National Academies Press, 2011.

14 Li T, Fan J, Wang B, Traugh N, Chen Q, Liu JS, *et al*. TIMER: a web server for comprehensive analysis of tumor-infiltrating immune cells. *Cancer Res* 2017; **77**:e108–e110.

15 Michielon E, Lopez Gonzalez M, Stolk DA, Stolwijk JGC, Roffel S, Waaijman T, *et al*. A reconstructed human melanoma-in-skin model to study immune modulatory and angiogenic mechanisms facilitating initial melanoma growth and invasion. *Cancers (Basel)* 2023; **15**:2849.

16 Wohlfeil SA, Hafele V, Dietsch B, Weller C, Sticht C, Jauch AS, *et al*. Angiogenic and molecular diversity determine hepatic melanoma metastasis and response to anti-angiogenic treatment. *J Transl Med* 2022; **20**:62.

17 Liu QH, Ma LS. Knockdown of thrombospondin 2 inhibits metastasis through modulation of PI3K signaling pathway in uveal melanoma cell line M23. *Eur Rev Med Pharmacol Sci* 2018; **22**:6230–6238.

18 Kim MJ, Sun HJ, Song YS, Yoo SK, Kim YA, Seo JS, *et al*. CXCL16 positively correlated with M2-macrophage infiltration, enhanced angiogenesis, and poor prognosis in thyroid cancer. *Sci Rep* 2019; **9**:13288.

19 Liu Y, Jiang C, Xu C, Gu L. Systematic analysis of integrated bioinformatics to identify upregulated THBS2 expression in colorectal cancer cells inhibiting tumour immunity through the HIF1A/lactic acid/GPR132 pathway. *Cancer Cell Int* 2023; **23**:253.

20 Carpino G, Cardinale V, Di Giamberardino A, Overi D, Donsante S, Colasanti T, *et al*. Thrombospondin 1 and 2 along with PEDF inhibit angiogenesis and promote lymphangiogenesis in intrahepatic cholangiocarcinoma. *J Hepatol* 2021; **75**:1377–1386.

21 Maiti A, Qi Q, Peng X, Yan L, Takabe K, Hait NC. Class I histone deacetylase inhibitor suppresses vasculogenic mimicry by enhancing the expression of tumor suppressor and anti-angiogenesis genes in aggressive human TNBC cells. *Int J Oncol* 2019; **55**:116–130.

22 Abed Kahnamouei S, Baghaei K, Pakzad P, Hashemi M, Zali MR. The role of extracellular matrix proteins in gastric cancer development via epithelial-mesenchymal transition. *Gastroenterol Hepatol Bed Bench* 2020; **13**:S139–S144.

23 Lee HJ, Park SW, Lee JH, Chang SY, Oh SM, Mun S, *et al*. Differential cellular origins of the extracellular matrix of tumor and normal tissues according to colorectal cancer subtypes. *Br J Cancer* 2025; **132**:770–782.

24 Barani A, Beikverdi K, Mashhadi B, Parsapour N, Rezaei M, Javid P, Azadeh M. Transcription analysis of the THBS2 gene through regulation by potential noncoding diagnostic biomarkers and oncogenes of gastric cancer in the ECM-receptor interaction signaling pathway: integrated system biology and experimental investigation. *Int J Genomics* 2023; **2023**:5583231.